ORIGINAL ARTICLE

Annals of Agricultural and Environmental Medicine
www.aaem.pl

OLMALINC alleviates dexamethasone-induced osteoporosis via targeting miR-124-3p

Siyuan Ha[1,A-B,D-E]*, Jing Xiao[2,B-C,F]*, Ning Gan[3,C,F], Huan Yang[3,C-D,F]

[1] *Anesthesiology, The Wuhan Hospital of TCM Affiliated to Hubei University of Traditional Chinese Medicine, Wuhan, China*
[2] *Endocrinology, Wuhan No.9 Hospital, Wuhan, China*
[3] *Orthopedics, The Wuhan Hospital of TCM Affiliated to Hubei University of Traditional Chinese Medicine, Wuhan, China*
A – Research concept and design, B – Collection and/or assembly of data, C – Data analysis and interpretation, D – Writing the article, E – Critical revision of the article, F – Final approval of the article

* Siyuan Ha and Jing Xiao contributed equally to this work.

Siyuan Ha, Jing Xiao, Ning Gan, Huan Yang. OLMALINC alleviates dexamethasone-induced osteoporosis via targeting miR-124-3p. Ann Agric Environ Med. Ann Agric Environ Med. doi:10.26444/aaem/215649

Abstract

Introduction and Objective. This study aims to investigate the mechanism of LncRNA(lncRNAs) OLMALINC in dexamethasone (Dex)-induced osteoblast differentiation impairment and osteoporosis.

Materials and Method. To investigate the impact of OLMALINC and miR-124-3p on Dex-treated osteoblasts, functional gain and loss experiments were conducted using MC3T3-E1 cells. Dual-luciferase reporter assays, RNA pull-down, and MS-RIP experiments were used to verify the targeting relationship between OLMALINC and miR-124-3p. RT-qPCR was conducted to analyze OLMALINC and miR-124-3p levels, as well as osteogenic regulatory factors OPG, Runx2, and ALP-related mRNA in different treatment groups. Protein expression levels were determined by Western blot analysis. Apoptosis was assessed by flow cytometry. cell viability was assessed by CCK-8.

Results. After Dex treatment, OLMALINC levels decreased, while miR-124-3p increased. Transfection of oe-OLMALINC counteracted Dex-induced osteogenic damage by increasing cell viability, decreasing apoptosis reduction, stimulating OPG, ALP, and Runx2 stimulation. OLMALINC targeted miR-124-3p, with OLMALINC negatively regulating miR-124-3p. In turn, miR-124-3p mimic reversed the protective effect of OLMALINC against Dex-induced osteoblast dysfunction.

Conclusions. These results indicate that the OLMALINC/miR-124-3p axis influences osteoblast differentiation in Dex-induced osteoblast differentiation impairment and osteoporosis by regulating cell viability, apoptosis, and osteogenic factors.

Key words

dexamethasone, osteoblastic differentiation, GIOP, OLMALINC, miR-124-3p

INTRODUCTION

Osteoporosis is a common bone disorder marked by a decrease in bone mass, reduced bone density, and deterioration in the structure of bone tissue [1, 2]. Hundreds of millions of people worldwide are affected, with China having the highest number of osteoporosis patients globally [3]. Glucocorticoids (GCs) are medications used to treat inflammation and autoimmune diseases [4], but long-term use of GCs has been reported as a significant risk factor for osteoporosis [5]. Dexamethasone (Dex), also a glucocorticoid anti-inflammatory drug [6, 7], can induce glucocorticoid-induced osteoporosis (GIOP) [8]. GIOP significantly increases the risk of fractures and osteonecrosis compared to traditional postmenopausal osteoporosis [9]. Therefore, exploring the molecular mechanisms of Dex-induced osteoporosis is of great significance.

Long non-coding RNAs (lncRNAs) are non-coding RNAs lacking open reading frames,.but are involved in various physiological and pathological processes of human diseases [10]. LncRNAs are also considered important regulators of osteoporosis, acting as key mediators between genetic predisposition and environmental influences [11]. For instance, studies have found that lncRNA Malat1 can bind to the Tead3 protein in macrophages-osteoclasts, inhibiting Nfatc1-mediated gene transcription and osteoclast differentiation, thereby preventing osteoporosis and bone metastasis [12]. LncRNAs are closely related to the mechanisms of bone resorption and formation mediated by osteoblasts and osteoclasts [13]. OLMALINC is a type of lncRNA, but its understanding is still limited. However, research has shown that OLMALINC is differentially expressed in the plasma of rheumatoid arthritis patients and has potential clinical value [14]. More importantly, it is recognized as an epigenetic diagnostic biomarker for osteoporosis risk and is significantly down-regulated in patients with low bone density [15]. Additionally, it has been reported to have good prognostic value in osteosarcoma [16]. Currently, however, there are no reports on the molecular mechanisms of OLMALINC in Dex-induced osteoporosis.

Based on the above background, we hypothesize that dysregulation of OLMALINC plays a pivotal role in the mechanisms underlying dexamethasone-induced osteoblast dysfunction and GIOP. The aim of the study is to elucidate the potential functions and mechanisms of OLMALINC in GIOP, with the goal of providing novel insights for the diagnosis and treatment of this disease.

✉ Address for correspondence: Huan Yang, Orthopedics, The Wuhan Hospital of TCM Affiliated to Hubei University of Traditional Chinese Medicine, Wuhan, China
E-mail: yanghuandr142@163.com

Received: 06.11.2025; accepted: 15.12.2025; first published: 02.02.2026

MATERIALS AND METHOD

Cell culture and treatment. This study employed the classic mouse pre-osteoblast cell line MC3T3-E1, which possesses stable osteogenic differentiation potential and is widely used in research on the mechanisms of osteoporosis [17]. Cells were maintained in DMEM enriched with 10% fetal bovine serum, along with 100 U/ml of penicillin and 100 μg/ml of streptomycin. The culture conditions were set at 37 °C with 5% carbon dioxide. Cells were medium-changed every 3 days and passaged when confluence reached 80–90%. To determine the optimal concentration of Dex, cells were co-incubated with Dex at different concentrations (0, 1, 2, 4 μM) for 24 h [18]. Ultimately, 4 μM was selected for subsequent cell model construction.

Cell transfection. An over-expression vector for OLMALINC (oe-OLMALINC) and a control group (oe-NC) were constructed using the pCDNA3.1 plasmid. Small interfering RNA (si-OLMALINC) targeting OLMALINC, miR-124-3p mimic, miR-124-3p inhibitor, and negative control groups (si-NC, mimic NC, inhibitor NC) were also constructed. The above vectors were transfected into cells using Lipofectamine 3000. Transfection for 48 h.

Cell viability. MC3T3-E1 cells were seeded in 96-well plates. The optimal dose of Dex was then determined using concentrations of 1, 2, and 4 μM. Briefly, CCK-8 solution was added to the cells at a ratio of 1:10, and they were incubated for 4 h. Finally, the OD value at 450 nm was measured using an ELX808 microplate reader.

Apoptosis. Apoptosis in MC3T3-E1 cells was detected using a dual staining method with Annexin V-FITC and PI. Briefly, the cells to be tested were collected into a centrifuge tube, stained with 5 μl Annexin V-FITC and 5 μl PI, washed with PBS after 30 min of staining, and analyzed for apoptosis using a FACSCalibur flow cytometer.

RT-qPCR. Total RNA was isolated and extracted from cultured MC3T3-E1 cells using TRIzol reagent. The extracted RNA was reverse transcribed into cDNA using the M-MLV Reverse Transcriptase kit, and qPCR was performed using a standard SYBR Green PCR kit on an Applied Biosystems 7300 Real-time PCR machine. The $2^{-\Delta\Delta Ct}$ method was used to evaluate the levels of OLMALINC, miR-107, miR-7-5p, miR-124-3p, miR-29a-3p, miR-29b-3p, miR-29c-3p, and miR-28-5p, as well as osteogenic-related genes OPG, ALP, and Runx2 mRNA. miRNA was normalized to U6, and lncRNA and mRNA were normalized to GAPDH. Primer sequences are shown in Supplementary Table S1.

Western blot analysis. Transfected MC3T3-E1 cells were lysed using RIPA buffer to extract total protein. Protein concentration was quantified using the BCA assay kit. Equal amounts of protein samples were separated by SDS-PAGE electrophoresis and transferred to PVDF membranes. After blocking with 5% skim milk powder, membranes were incubated overnight at 4 °C with the following primary antibodies: anti-OPG, anti-ALP, anti-Runx2, and anti-GAPDH. The Following primary antibody incubation, membranes were incubated with HRP-labeled secondary antibody at room temperature for 2 h. Protein bands were visualized using enhanced chemiluminescence (ECL) substrate and imaged with the Bio-Rad ChemiDoc system. Band intensities were quantified using Image Lab software. Uncropped blots are provided in Supplementary Figures S1 and S2.

Supplementary Table S1. Primer sequences used for RT-qPCR

RNA	Primer sequence (5′-3′)
OLMALINC	Forward GACTCCTTTGGGAGACCAGTG
	Reverse AGGTCACAGGGGATTTGATGG
miR-124-3p	Forward ACACTCCAGCTGGGTAAGGCACGCGGTGAA
	Reverse CTCAACTGGTGTCGTGGAGTCGGCAATTCAGTTGAGGGCATTCAC
miR-7-5p	Forward ACACTCCAGCTGGGTGGAAGACTAGTAGTTTT
	Reverse CTCAACTGGTGTCGTGGAGTCGGCAATTCAGTTGAGAACAACAA
miR-29a-3p	Forward AGCACCAUCUGAAAUCGGUU
	Reverse GTGCAGGGTCCGAGGT
miR-29b-3p	Forward CGCGTAGCACCATTTGAAATC
	Reverse AGTGCAGGGTCCGAGGTATT
miR-29c-3p	Forward ACACTGCTCCAGGGTAGCACCATTTGAAAT
	Reverse TGGTGTCGTGGAGTCG
miR-28-5p	Forward GCGCATTGCACTTGTCTCG
	Reverse AGTGCAGGGTCCGAGGTATT
miR-107	Forward AGCAGCATTGTACAGGG
	Reverse GTGCAGGGTCCGAGGT
OPG	Forward TGCTGTTCCTACAAAGTTTACG
	Reverse CTTTGAGTGCTTTAGTGCGTG
ALP	Forward ATTTCTCTTGGGCAGGCAGAGAGT
	Reverse ATCCAGAATGTTCCACGGAGGCTT
Runx2	Forward TCTTAGAACAAATTCTGCCCTTT
	Reverse TGCTTTGGTCTTGAAATCACA
GAPDH	Forward TGTTCGTCATGGGTGTGAAC
	Reverse ATGGCATGGACTGTGGTCAT
U6	Forward CTCGCTTCGGCAGCACA
	Reverse AACGCTTCACGAATTTGCGT

Bioinformatics analysis. OLMALINC target miRNA predictions were conducted using the online databases DIANA, lncRNASNP2, and LncBook, selecting overlapping predicted results as candidate targets for OLMALINC.

Dual-Luciferase assay. The binding sites of OLMALINC and miR-124-3p were predicted using the lncRNASNP2 online database. Wild-type (WT-OLMALINC) and mutant (MUT-OLMALINC) plasmids were constructed using the pmirGLO vector. MC3T3-E1 cells were co-transfected with miR-124-3p mimic, miR-124-3p inhibitor, and mimic NC, inhibitor NC along with the above plasmids. After 48 h, the luciferase activity of OLMALINC was measured using a dual-luciferase reporter assay system.

MS2-RIP. MC3T3-E1 cells were co-transfected with pcDNA3.1-MS2, pcDNA3.1-MS2-OLMALINC, or pcDNA3.1-MS2-OLMALINC-mut and pMS2-GFP. After 48 h of transfection, RIP detection was performed using a GFP antibody and Magna RIP™ RNA-binding protein

Supplementary Table S2. Detailed results of statistical analysis

Comparison Group	*P*	95% CI	η^2
Fig. 1A			0.936
0 vs. 1	0.0002	8.73 - 26.63	
0 vs. 2	<0.0001	20.07 - 37.97	
0 vs. 4	<0.0001	37.69 - 55.59	
Fig. 1B			0.768
0 vs. 7	0.0173	–1.18 - –0.12	
0 vs. 14	0.0001	–1.78 - –0.73	
Fig. 1C			0.813
0 vs. 1	0.0369	0.01 – 0.41	
0 vs. 2	0.0004	0.17 – 0.57	
0 vs. 4	<0.0001	0.36 – 0.76	
Fig. 2A			0.905
oe-NC vs. oe-OLMALINC	<0.0001	–2.30 - –1.27	
Fig. 2B			0.822
Control vs. Dex	0.0002	0.28 - 0.84	
Dex + oe-NC vs. Dex + oe- OLMALINC	<0.0001	–0.92 - –0.36	
Fig. 2C			0.814
Control vs. Dex	<0.0001	0.99-1.63	
Dex + oe-NC vs. Dex + oe- OLMALINC	<0.0001	–1.06 - –0.42	
Fig. 2D			0.895
Control vs. Dex	<0.0001	–28.15 - –14.58	
Dex + oe-NC vs. Dex + oe- OLMALINC	<0.0001	10.43 – 24.01	
Fig. 2E			0.811
Control vs. Dex	0.0004	0.25 - 0.85	
Dex + oe-NC vs. Dex + oe- OLMALINC	<0.0001	–0.97 - –0.37	
Fig. 2F			0.749
Control vs. Dex	0.0013	0.17 – 0.69	
Dex + oe-NC vs. Dex + oe- OLMALINC	0.0006	–0.73 - –0.21	
Fig. 2G			0.566
Control vs. Dex	0.0180	0.07 – 0.85	
Dex + oe-NC vs. Dex + oe- OLMALINC	0.0331	–0.81 - –0.03	
Fig. 3C			0.923
Control vs. Dex	<0.0001	–1.00 - –0.62	
Fig. 3D			0.740
Control vs. Dex	0.0014	–0.79 - –0.28	
Fig. 3E			0.752
Control vs. Dex	0.0012	–0.81 - –0.29	
Fig. 3F			0.704
Control vs. Dex	0.0024	–0.65 - –0.20	
Fig. 3G			0.114
Control vs. Dex	0.3399	–0.43 - –0.17	
Fig. 3H			0.768
Control vs. Dex	0.0009	0.40 - 1.05	
Fig. 3I			0.555
Control vs. Dex	0.0135	0.11 - 0.72	
Fig. 4B			0.638
mimic NC vs. miR-124-3p mimic	0.0007	0.20 – 0.93	
inhibitor NC vs. miR-124-3p inhibitor	<0.0001	–1.28 - –0.55	
Fig. 4D			0.981
MS2-OLMALINC vs. MS2-OLMALINC-mut	<0.0001	10.10 - 12.93	
Fig. 4E			0.943
WT-bio-miR-124-3p vs. MUT-bio-miR-124-3p	<0.0001	1.34 - 2.06	
Fig. 4F			0.963
oe-NC vs. oe-OLMALINC	<0.0001	0.45 - 0.74	
si-NC vs. si-OLMALINC	<0.0001	–0.60 - –0.30	
Fig. 5A			0.828
Control vs. Dex	<0.0001	0.31 - 0.89	
Dex + oe-NC vs. Dex + oe-OLMALINC	<0.0001	–0.96 - –0.37	
Dex+oe-OLMALINC+mimic NC vs. Dex+oe-OLMALINC+miR-124-3p mimic	0.6968	–0.15 - –0.43	
Fig. 5B			0.978
Control vs. Dex	<0.0001	–1.47 - –1.07	
Dex + oe-NC vs. Dex + oe-OLMALINC	<0.0001	1.13 - 1.53	
Dex+oe-OLMALINC+mimic NC vs. Dex+oe-OLMALINC+miR-124-3p mimic	<0.0001	–1.22 - –0.82	
Fig. 5C			0.836
Control vs. Dex	<0.0001	–1.05 - –1.77	
Dex + oe-NC vs. Dex + oe-OLMALINC	<0.0001	–1.27 - –0.55	
Dex+oe-OLMALINC+mimic NC vs. Dex+oe-OLMALINC+miR-124-3p mimic	<0.0001	0.21 - –0.93	
Fig. 5D			0.921
Control vs. Dex	<0.0001	–27.96 - –16.48	
Dex + oe-NC vs. Dex + oe-OLMALINC	<0.0001	11.85 - 23.34	
Dex+oe-OLMALINC+mimic NC vs. Dex+oe-OLMALINC+miR-124-3p mimic	<0.0001	–17.60 - –6.12	
Fig. 5E			0.805
Control vs. Dex	0.0022	0.18 - –1.02	
Dex + oe-NC vs. Dex + oe-OLMALINC	<0.0001	–1.38 - –0.54	
Dex+oe-OLMALINC+mimic NC vs. Dex+oe-OLMALINC+miR-124-3p mimic	0.0076	0.11 - 0.95	
Fig. 5F			0.748
Control vs. Dex	0.0003	0.23 - 0.90	
Dex + oe-NC vs. Dex + oe-OLMALINC	0.0003	–0.90 - –0.23	
Dex+oe-OLMALINC+mimic NC vs. Dex+oe-OLMALINC+miR-124-3p mimic	0.0101	0.08 - 0.75	
Fig. 5F			0.684
Control vs. Dex	0.0007	0.19 - 0.82	
Dex + oe-NC vs. Dex + oe-OLMALINC	0.0058	–0.74 - –0.10	
Dex+oe-OLMALINC+mimic NC vs. Dex+oe-OLMALINC+miR-124-3p mimic	0.0287	0.03 – 0.66	

immunoprecipitation reagent, with anti-GFP and control IgG used for MS2-RIP detection. The purified RNA was quantified using RT-qPCR.

RNA pull-down. Biotin labelling was performed using a combination of biotin RNA label and T7 RNA polymerase, including WT-bio-miR-124-3p, MUT-bio-miR-124-3p, and NC-bio-probe. The lysate from MC3T3-E1 cells was incubated with the above biotin-conjugated probes, followed by incubation with magnetic beads for 2 h. The miR-124-3p-related complexes were separated using the RNeasy Mini Kit, and then extracted using Trizol for RT-qPCR.

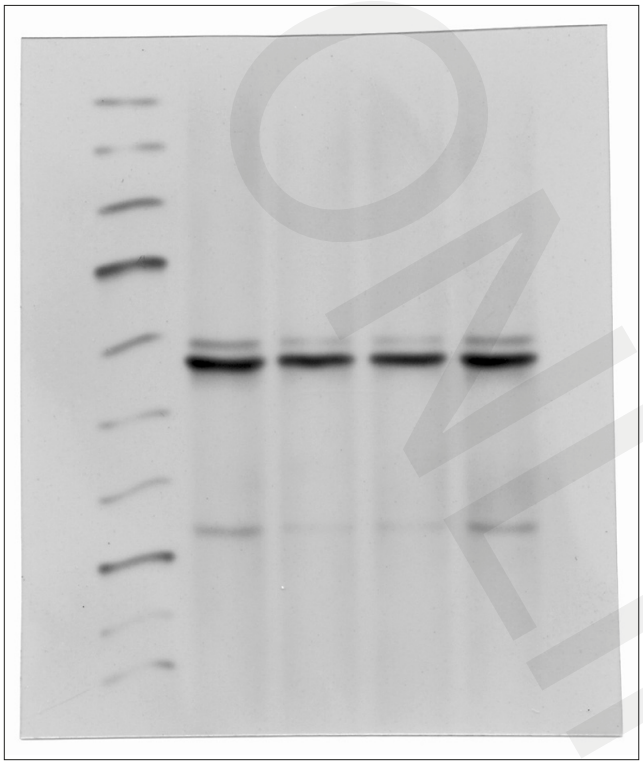

ALP

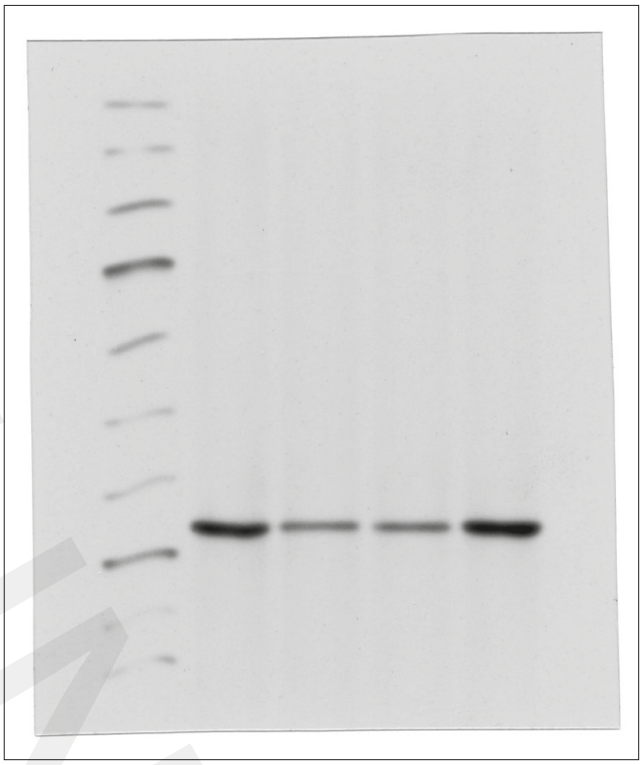

OPG

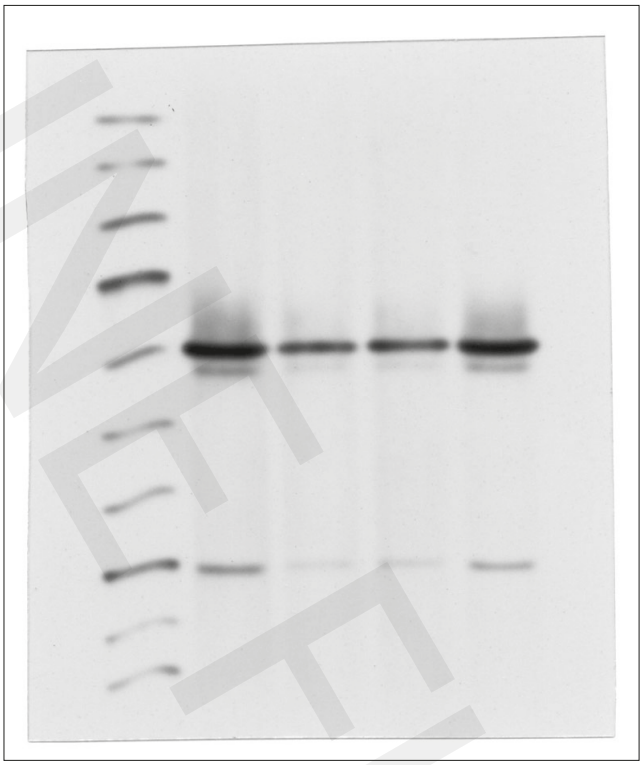

Runx2

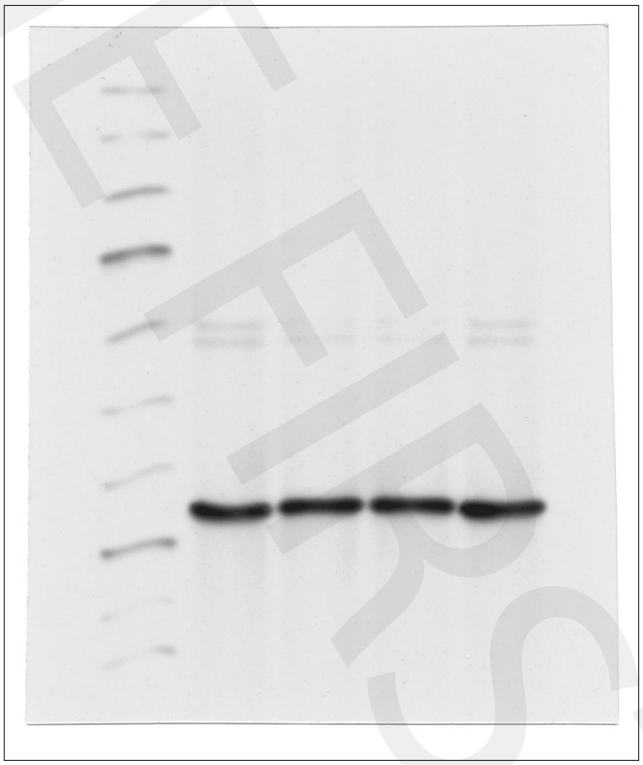

GAPDH

Supplementary Figure S1. Uncropped original Western blot analysis of osteopontin expression in Dex-induced MC3T3-E1 cells over-expressing OLMALINC

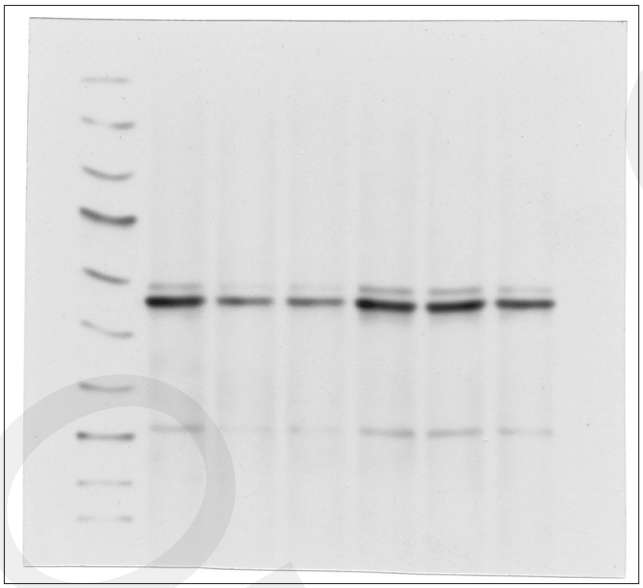

ALP

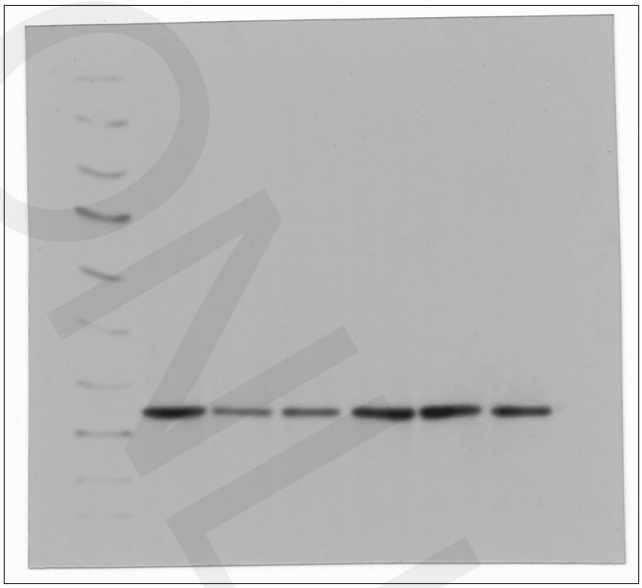

OPG

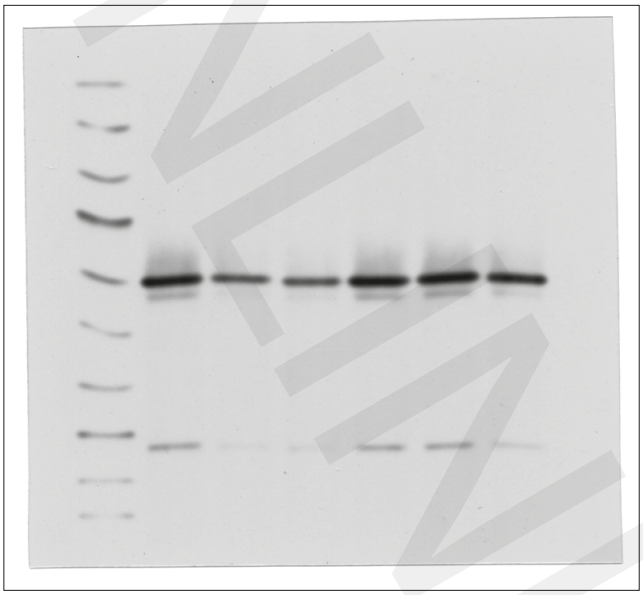

Runx2

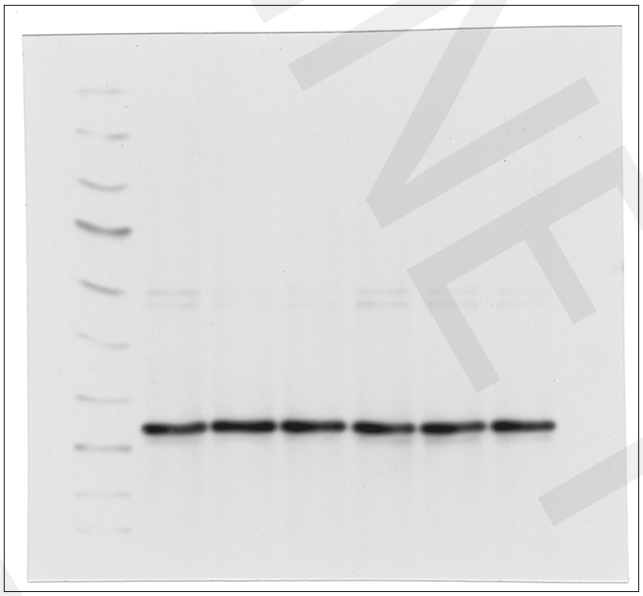

GAPDH

Supplementary Figure S2. Uncropped original Western blot analysis of osteopontin expression in Dex-induced MC3T3-E1 cells over-expressing OLMALINC and transfection with miR-124-3p mimic

Data analysis. All data were analyzed using GraphPad Prism 9. Data were obtained from at least three independent experiments and presented as mean ± SD. Comparisons between two groups were performed using Student's t-test, while multiple group comparisons (at least three groups) were conducted using one-way ANOVA, followed by Tukey's *post hoc* test for multiple comparisons. $P < 0.05$ was considered statistically significant. For all analyses, effect sizes, 95% confidence intervals (95% CI), and exact p-values are detailed in Supplementary Table S2.

RESULTS

Down-regulation of OLMALINC in Dex-treated MC3T3-E1 cells. First, OLMALINC levels in Dex-treated MC3T3-E1 cells were assessed using RT-qPCR. It was initially observed that cell viability significantly decreased as the concentration of Dex increased ($P<0.001$) (Fig. 1A). As shown in OLMALINC levels increased significantly over time during osteogenic differentiation ($P<0.05$) (Fig. 1B). However, treatment with Dex noticeably inhibited OLMALINC expression ($P<0.05$) (Fig. 1C).

Over-expression of OLMALINC antagonized the inhibitory efffects of Dex on osteoblast differentiation. To investigate the role of OLMALINC in osteoblast

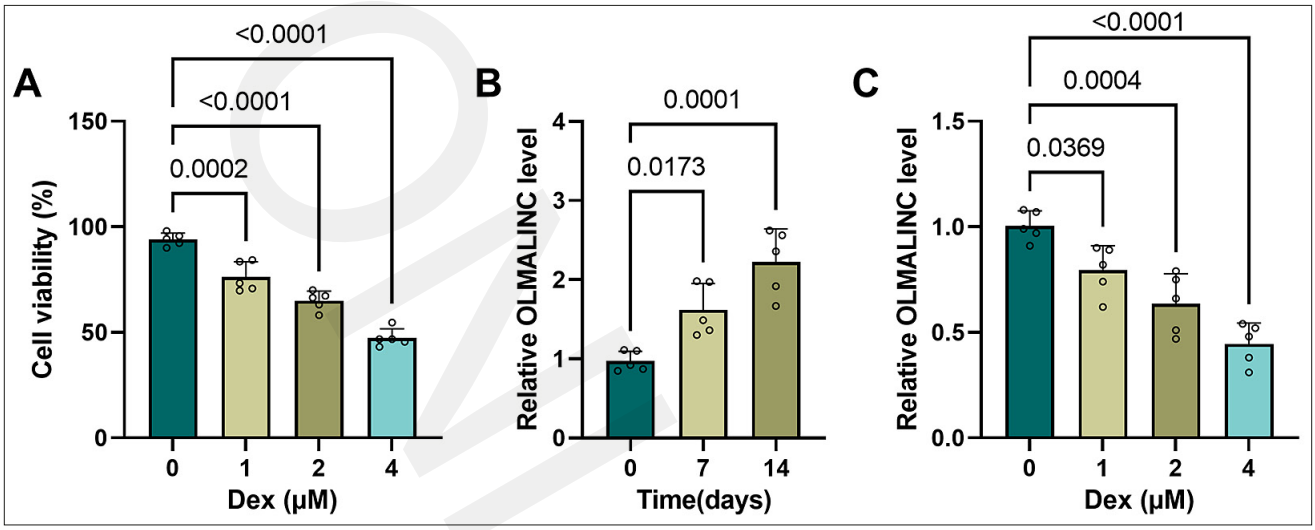

Figure 1. OLMALINC levels in Dex-treated MC3T3-E1 cells. (A) Cell viability decreased as the concentration of Dex increased. (B) OLMALINC levels increased with the duration of osteogenic treatment. (C) OLMALINC levels decreased as the concentration of Dex increased.
Data are presented as mean ± SD (n = 5 biological replicates, each with 3 technical replicates). Statistical significance was determined by one-way ANOVA with Tukey's *post-hoc* test

differentiation, MC3T3-E1 cells were transfected with oe-OLMALINC ($P<0.0001$) (Fig. 2A). Following transfection, the reduced expression level of OLMALINC due to Dex treatment was significantly rebounded ($P<0.001$) (Fig. 2B). Following Dex treatment, cell viability decreased, and apoptosis was stimulated; however, over-expression of OLMALINC alleviated the decline in cell viability and the increase in apoptosis ($P<0.0001$) (Fig. 2C and D). Dex treatment significantly reduced levels of OPG, ALP, and Runx2 in MC3T3-E1 cells ($P<0.05$) (Fig. 2E). In contrast, overexpression of OLMALINC significantly upregulated OPG, ALP, and Runx2 ($P<0.05$) (Fig. 2E).

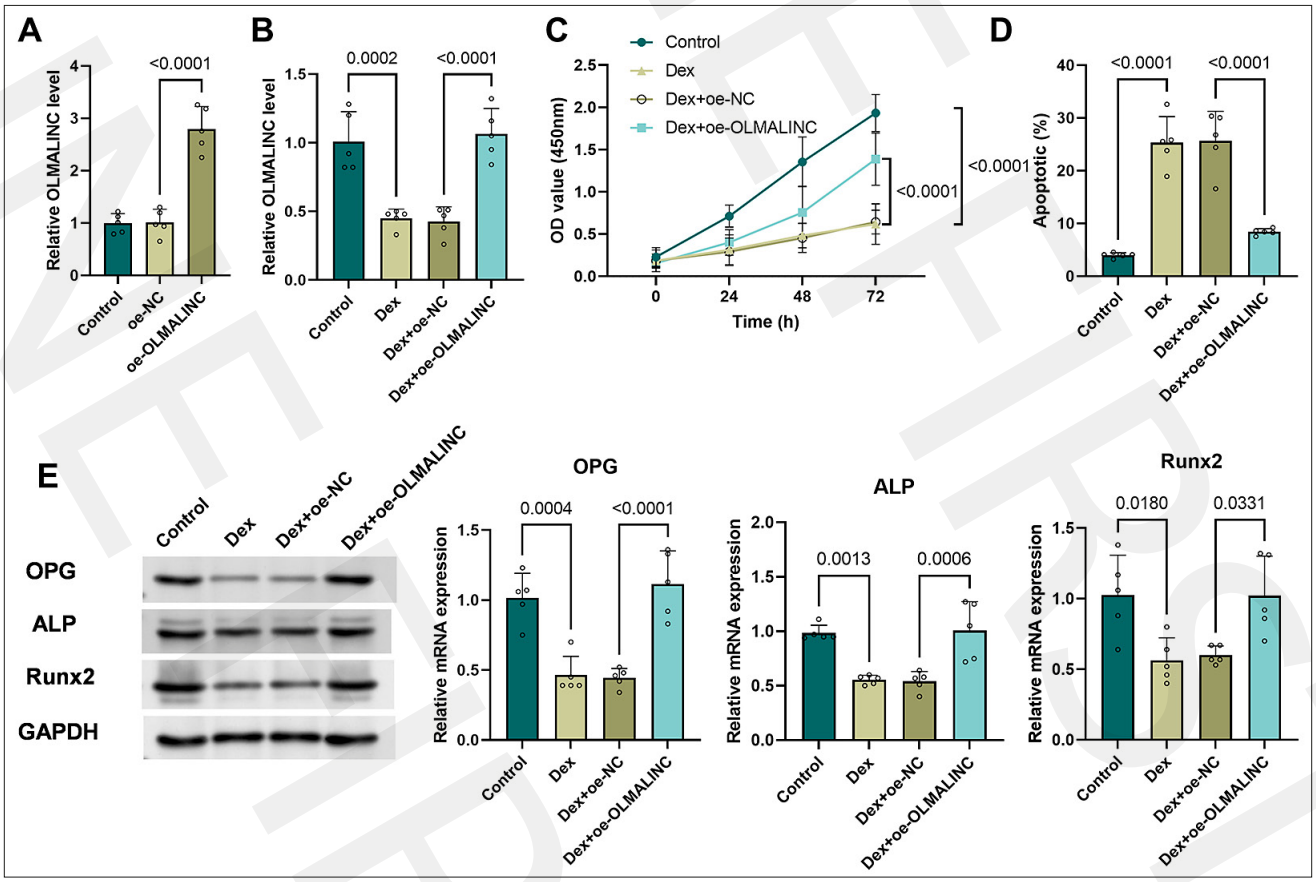

Figure 2. Effects of OLMALINC over-expression on Dex-treated MC3T3-E1 cells. (A) Successful transfection of oe-OLMALINC. Transfection with oe-OLMALINC affected OLMALINC levels (B), as well as cell viability (C), apoptosis (D), and levels of OPG, ALP, and Runx2 (E) in Dex-treated MC3T3-E1 cells.
Data are presented as mean ± SD (n = 5 biological replicates, each with 3 technical replicates). Statistical significance was determined by one-way ANOVA with Tukey's *post-hoc* test

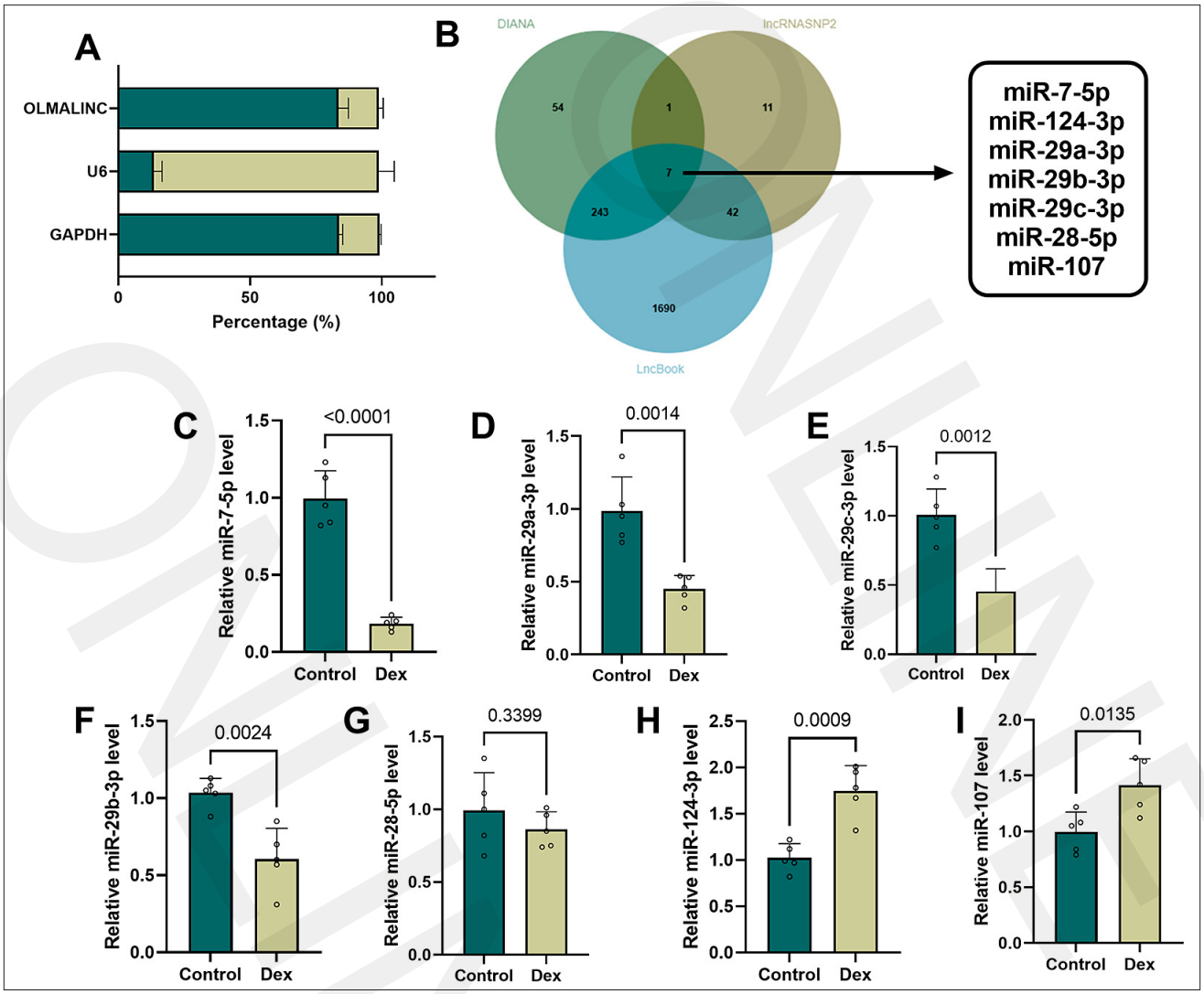

Figure 3. Analysis of the target miRNAs of OLMALINC. (A) Subcellular localization analysis of OLMALINC. (B) Venn diagram of target miRNAs of OLMALINC. The levels of potential target miRNAs, including miR-7–5p (C), miR-29a-3p (D), miR-29c-3p (E), miR-29b-3p (F), miR-28–5p (G), miR-124–3p (H), and miR-107 (I), were assessed in Dex-treated MC3T3-E1 cells.
Data are presented as mean ± SD (n = 5 biological replicates, each with 3 technical replicates). Statistical significance was determined by two-tailed Student's t-test

Target miRNA analysis of OLMALINC. The lncLocator online database showed that OLMALINC is predominantly enriched in the cytoplasm, a prediction supported by subcellular localization analysis (Fig. 3A). This confirmed that OLMALINC had the prerequisites to function as a ceRNA. We also predicted the target miRNAs of OLMALINC using the online databases DIANA, lncRNASNP2, and LncBook, identifying seven potential binding partners: miR-107, miR-7-5p, miR-124-3p, miR-29a-3p, miR-29b-3p, miR-29c-3p, and miR-28-5p (Fig. 3B). To identify the specific downstream miRNAs of OLMALINC in MC3T3-E1 cells, RT-qPCR on Dex-treated osteoblasts was conducted. Among the seven candidate miRNAs examined, miR-124-3p exhibited the most significant upregulation ($P < 0.001$) (Fig. 3C-I). Therefore, miR-124-3p was selected as the primary target for subsequent investigation.

Analysis of the interaction between OLMALINC and miR-124-3p. The lncRNASNP2 online database predicted the binding sites of OLMALINC and miR-124-3p (Fig. 4A). Dual-luciferase assays confirmed that miR-124-3p mimic suppressed, while its inhibitor enhanced, the activity of wild-type OLMALINC reporter ($P < 0.001$) (Fig. 4B), with no effect on the mutant ($P > 0.05$) (Fig. 4B). Subsequent MS2-RIP and RNA pull-down assays verified their direct physical interaction ($P < 0.0001$) (Fig. 4D-E). Moreover, OLMALINC overexpression decreased, while its knockdown increased, miR-124-3p levels ($P < 0.0001$) (Fig. 4F). These findings collectively demonstrate that OLMALINC functions as a molecular sponge for miR-124-3p.

Role of the OLMALINC/miR-124-3p axis in Dex-treated MC3T3-E1 cell. Having confirmed the direct interaction, we examined the functional relevance of the OLMALINC/miR-124-3p axis. As shown in Fig. 5A-B, Dex down-regulated OLMALINC expression and up-regulated miR-124-3p. Transfection with oe-OLMALINC increased OLMALINC expression and decreased miR-124-3p, whereas co-transfection with a miR-124-3p mimic restored miR-124-3p levels ($P < 0.0001$). Furthermore, the transfection of miR-124-3p mimic reversed the protective effect of OLMALINC against Dex-induced osteoblast dysfunction and apoptosis.

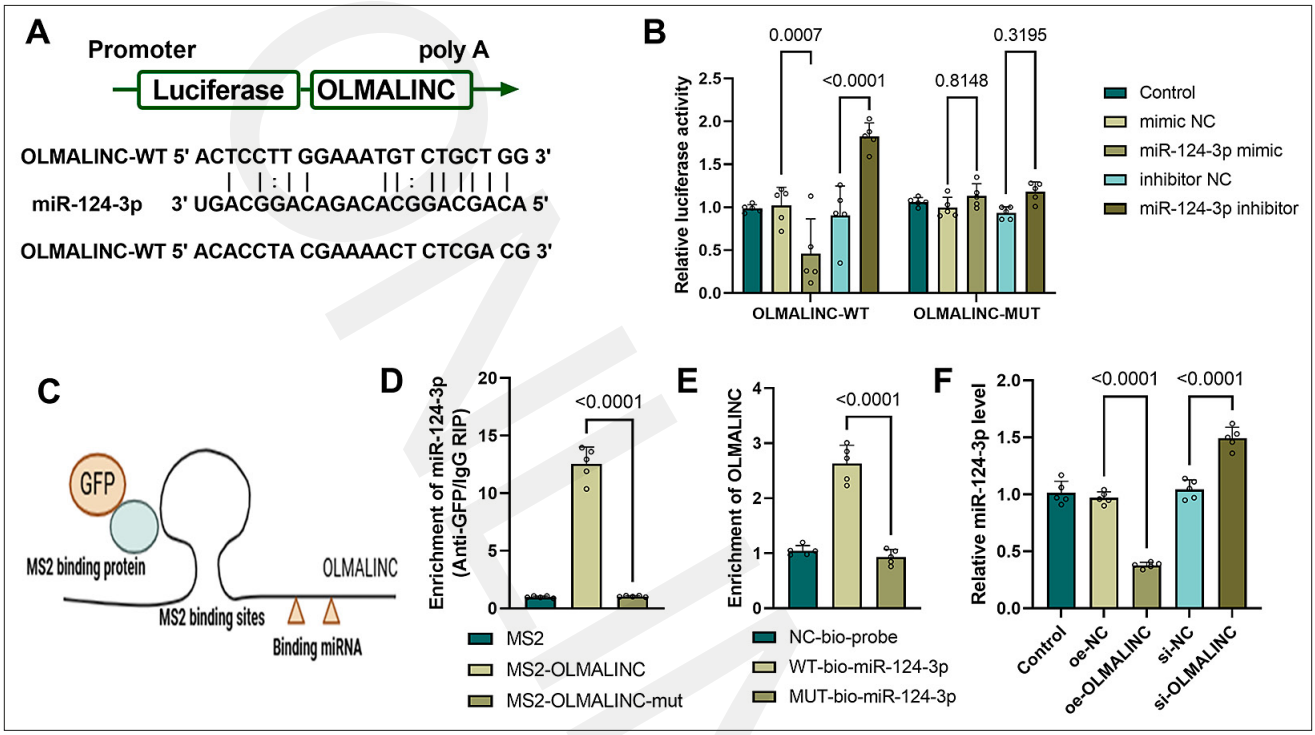

Figure 4. OLMALINC targeted miR-124–3p. (A) Binding sites of OLMALINC and miR-124–3p. (B) Dual-luciferase reporter assay. (C) Schematic diagram of the MS2-RIP experiment. (D) Results of the MS2-RIP experiment. (E) RNA pull-down experiment. (F) Modulation of the effect of OLMALINC on miR-124–3p levels.
Data are presented as mean ± SD (n = 5 biological replicates, each with 3 technical replicates). Statistical significance was determined by one-way ANOVA with Tukey's *post-hoc* test

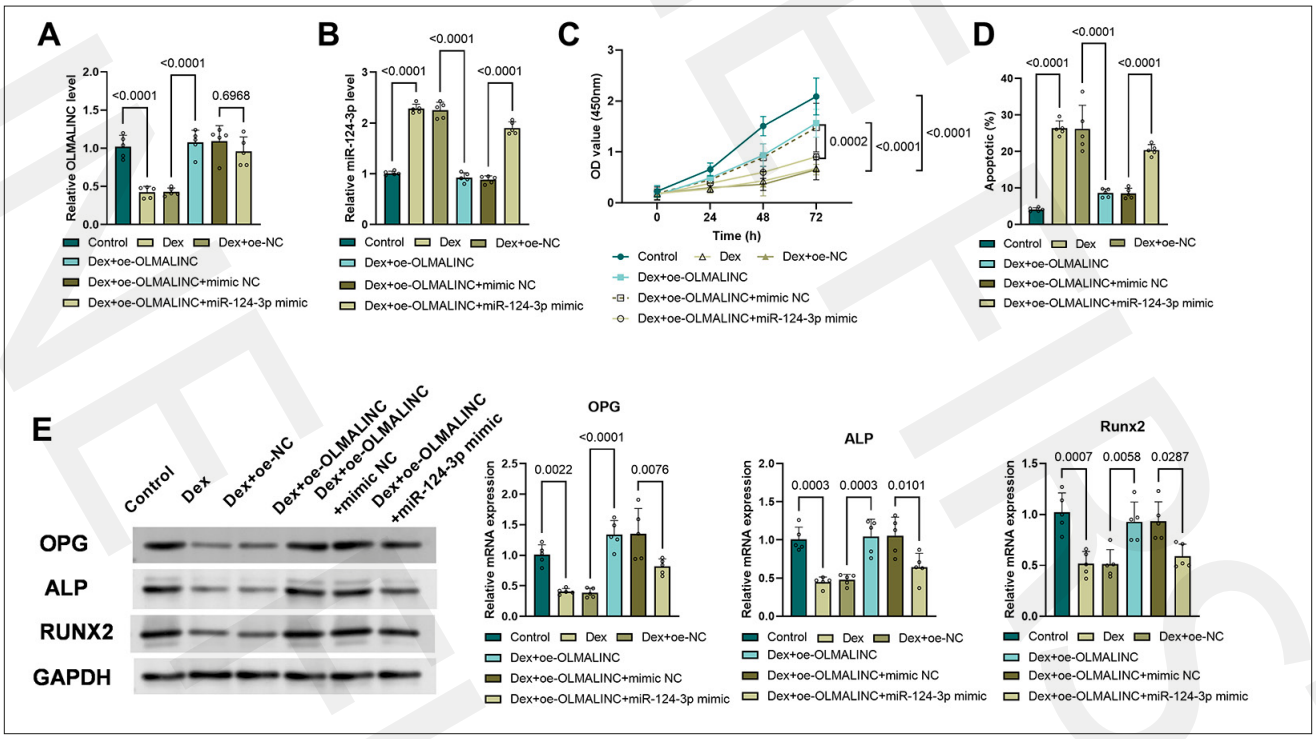

Figure 5. The role of the OLMALINC/miR-124–3p axis in Dex-treated MC3T3-E1 cells. Effects of modulating OLMALINC and miR-124–3p on OLMALINC (A) and miR-124–3p levels (B), as well as cell viability (C), apoptosis (D), and levels of OPG, ALP, and Runx2 (E).
Data are presented as mean ± SD (n = 5 biological replicates, each with 3 technical replicates). Statistical significance was determined by one-way ANOVA with Tukey's *post-hoc* test

After over-expression of miR-124-3p, cell viability declined again, and apoptosis increased ($P < 0.001$) (Fig. 5C and D). More importantly, miR-124-3p mimic resulted in decreased levels of OPG, ALP, and Runx2 ($P < 0.05$) (Fig. 5E), thus antagonizing the positive effects of oe-OLMALINC on Dex-induced osteoblast dysfunction.

DISCUSSION

The formation and progression of osteoporosis is primarily attributed to decreased bone formation [19]. Osteoporosis can be classified into two types: primary osteoporosis and secondary osteoporosis, which is caused by diseases or medications that affect bone metabolism[20], such as Dex. After the onset of osteoporosis, the number of trabecular bones decreases, and bone brittleness increases, leading to fractures even under minor external forces [21, 22]. This significantly reduces the quality of life for patients. Although there is a substantial population of osteoporosis patients in China, the diagnosis and management of the condition remain suboptimal [23]. Therefore, exploring the mechanisms of osteoporosis is crucial.

In recent years, the complex relationship between ncRNAs and diseases has garnered significant attention [24]. Recent technological innovations have further facilitated the functional characterization and mechanistic understanding of disease-related lncRNAs [25]. The role of lncRNAs in bone metabolic diseases, particularly osteoporosis, has also received increasing attention. Recent studies have found that lncRNAs RAD51-AS1, SNHG14, and GM15416 promote osteoblast differentiation through different pathways, alleviating the progression of osteoporosis [26]. This study confirms that OLMALINC levels increase with osteogenic differentiation time and are suppressed following Dex treatment. Furthermore, the findings of the current study indicate that OLMALINC alleviates Dex-induced osteogenic differentiation impairment by reducing osteoblast apoptosis, protecting cell viability, and promoting osteoblast markers. Zhu et al. also found that OLMALINC enhances the osteogenic differentiation of renal interstitial fibroblasts [27]. To further explore the mechanisms by which OLMALINC participates in Dex-induced osteogenic impairment and osteoporosis, we analyzed the downstream target miRNAs of OLMALINC.

Using the DIANA, lncRNASNP2, and LncBook online databases, seven potential binding partners for OLMALINC were predicted. RT-qPCR analysis of Dex-treated osteoblasts revealed that miR-124-3p exhibited the greatest upregulation. This discovery is consistent with earlier studies that indicate miR-124-3p is notably upregulated in mesenchymal stem cells from osteoporotic bone marrow [28]. Additionally, there are reports that miR-124-3p can inhibit osteogenic differentiation by inactivating the PI3K/Akt/mTOR pathway [29]. Therefore, we chose miR-124-3p as the primary target of OLMALINC for further study. First, we used experiments such as RIP to confirm the direct interaction between OLMALINC and miR-124-3p. We then explored the role of the OLMALINC/miR-124-3p axis in Dex-induced osteogenic impairment through gain-of-function experiments. The current study found that transfection with miR-124-3p mimic partially reversed the protective effects of OLMALINC on osteogenic differentiation, as evidenced by decreased cell viability, increased apoptosis, and a decline in OPG, ALP, and Runx2 levels. This aligns with findings of Gu et al., who demonstrated that miR-124-3p over-expression partially reverses the promotion of osteogenic differentiation by MALAT1 through regulation of IGF2BP1 [30]. Further studies indicate that in diabetic osteoporosis models, miR-124-3p modulates osteogenic activity via the GSK-3β/β-catenin signalling axis [31]. The convergence of these findings strongly suggests that miR-124-3p may play a pivotal role in bone homeostasis regulation by participating in multiple signalling pathways.

The presented study preliminarily revealed the role of the OLMALINC/miR-124-3p axis in Dex-induced osteoblast injury through *in vitro* experiments. However, the following limitations remain: First, all experiments were conducted using the mouse MC3T3-E1 cell line, and the results require *in vivo* validation in animal models that more closely mimic physiological conditions. Second, miR-124-3p possesses a complex regulatory network in bone metabolism and may influence osteogenic differentiation through multiple signaling pathways (e.g., GSK-3β/β-catenin). This study has not yet elucidated its specific downstream targets and pathway mechanisms in this model. Furthermore, as current research primarily utilizes mouse cell models, the translation of these findings to the pathophysiological processes of human osteoporosis requires further cautious evaluation. Future research will focus on establishing a glucocorticoid-induced GIOP animal model to validate the biological function of the OLMALINC/miR-124-3p axis in vivo and systematically elucidate its downstream signalling regulatory network. This will provide a more comprehensive evidence base for studying the mechanisms and potential interventions involving this target in GIOP.

In summary, the presented study confirmed that lncRNA OLMALINC is upregulated during osteogenic differentiation but suppressed by Dex. OLMALINC can promote osteoblast differentiation by protecting cell viability, reducing apoptosis, and stimulating osteogenic markers, thereby counteracting Dex-induced osteogenic impairment and GIOP. And its function is mediated through the miRNA-124-3p pathway. These findings provide new insights into the intrinsic mechanisms of GIOP.

REFERENCES

1. Figliomeni A, Signorini V, Mazzantini M. One year in review 2018: progress in osteoporosis treatment. Clin Exp Rheumatol. 2018;36(6):948–58.
2. Lis-Studniarska D, Studniarski M, Zakrzewska A, et al. Determining the hierarchy of risk factors for low-energy fractures in patients of an Osteoporosis Treatment Clinic. Ann Agric Environ Med. 2024;31(3):401–9.
3. Chen Y, Sun Y, Xue X, et al. Comprehensive analysis of epigenetics mechanisms in osteoporosis. Front Genet. 2023;14:1153585.
4. Paglialunga M, Flamini S, Contini R, et al. Anti-Inflammatory Effects of Synthetic Peptides Based on Glucocorticoid-Induced Leucine Zipper (GILZ) Protein for the Treatment of Inflammatory Bowel Diseases (IBDs). Cells. 2023;12(18).
5. Xiao J, Li W, Li G, et al. STK11 overexpression prevents glucocorticoid-induced osteoporosis via activating the AMPK/SIRT1/PGC1alpha axis. Hum Cell. 2022;35(4):1045–59.
6. Han X, Bai F, Li P, et al. Identification of novel potential drugs for the treatment and prevention of osteoarthritis. Biochem Biophys Rep. 2024;37:101647.
7. Szudy-Szczyrek A, Chocholska S, Bachanek-Mitura O, et al. Efficacy of ixazomib-lenalidomide-dexamethasone in high-molecular-risk

relapsed/refractory multiple myeloma – case series and literature review. Ann Agric Environ Med. 2022;29(1):103–9.
8. Mitra R. Adverse effects of corticosteroids on bone metabolism: a review. PM R. 2011;3(5):466–71; quiz 71.
9. Zheng X, Ye FC, Sun T, et al. Delay the progression of glucocorticoid-induced osteoporosis: Fraxin targets ferroptosis via the Nrf2/GPX4 pathway. Phytother Res. 2024;38(11):5203–24.
10. Fan H, Zhou Y, Zhang Z, et al. ROR1-AS1: A Meaningful Long Noncoding RNA in Oncogenesis. Mini Rev Med Chem. 2024;24(21):1884–93.
11. Baniasadi M, Talebi S, Mokhtari K, et al. Role of non-coding RNAs in osteoporosis. Pathol Res Pract. 2024;253:155036.
12. Zhao Y, Ning J, Teng H, et al. Long noncoding RNA Malat1 protects against osteoporosis and bone metastasis. Nat Commun. 2024;15(1):2384.
13. Yang Y, Yujiao W, Fang W, et al. The roles of miRNA, lncRNA and circRNA in the development of osteoporosis. Biol Res. 2020;53(1):40.
14. Shuai ZQ, Wang ZX, Ren JL, et al. Differential expressions and potential clinical values of lncRNAs in the plasma exosomes of rheumatoid arthritis. Int Immunopharmacol. 2024;128:111511.
15. Zhang M, Cheng L, Zhang Y. Characterization of Dysregulated lncRNA-Associated ceRNA Network Reveals Novel lncRNAs With ceRNA Activity as Epigenetic Diagnostic Biomarkers for Osteoporosis Risk. Front Cell Dev Biol. 2020;8:184.
16. He Y, Zhou H, Xu H, et al. Construction of an Immune-Related lncRNA Signature That Predicts Prognosis and Immune Microenvironment in Osteosarcoma Patients. Front Oncol. 2022;12:769202.
17. Dai X, Liu C, Bi W, et al. Estradiol and vitamin D exert a synergistic effect on preventing osteoporosis via the miR-351-5p/IRS1 axis and mTOR/NFkappaB signaling pathway. Sci Rep. 2025;15(1):18678.
18. Wang N, Wang H, Chen J, et al. ACY-1215, a HDAC6 inhibitor, decreases the dexamethasone-induced suppression of osteogenesis in MC3T3-E1 cells. Mol Med Rep. 2020;22(3):2451–9.
19. Lee S, Kim M, Hong S, et al. Effects of Sparganii Rhizoma on Osteoclast Formation and Osteoblast Differentiation and on an OVX-Induced Bone Loss Model. Front Pharmacol. 2021;12:797892.
20. Zhan W, Ruan B, Dong H, et al. Isopsoralen suppresses receptor activator of nuclear factor kappa-beta ligand-induced osteoclastogenesis by inhibiting the NF-kappaB signaling. PeerJ. 2023;11:e14560.
21. Kaczmarczyk-Sedlak I, Wojnar W, Zych M, et al. Effect of formononetin on mechanical properties and chemical composition of bones in rats with ovariectomy-induced osteoporosis. Evid Based Complement Alternat Med. 2013;2013:457052.
22. Ille M, Matic S, Gambiroza K, et al. Assessment of post-traumatic arthritis and functional outcome in patients treated operatively and non-operatively for distal radius Fractures – a 2-year cohort study. Ann Agric Environ Med. 2025;32(2):288–94.
23. Zhang H, Wei W, Qian B, et al. Screening for osteoporosis based on IQon spectral CT virtual low monoenergetic images: Comparison with conventional 120 kVp images. Heliyon. 2023;9(10):e20750.
24. Nemeth K, Bayraktar R, Ferracin M, et al. Non-coding RNAs in disease: from mechanisms to therapeutics. Nat Rev Genet. 2024;25(3):211–32.
25. Wang G, Lee-Yow Y, Chang HY. Approaches to probe and perturb long noncoding RNA functions in diseases. Curr Opin Genet Dev. 2024;85:102158.
26. Li B, Wang J, Xu F, et al. LncRNA RAD51-AS1 Regulates Human Bone Marrow Mesenchymal Stem Cells via Interaction with YBX1 to Ameliorate Osteoporosis. Stem Cell Rev Rep. 2023;19(1):170–87.
27. Zhu Z, Huang F, Jiang Y, et al. OLMALINC/OCT4/BMP2 axis enhances osteogenic-like phenotype of renal interstitial fibroblasts to participate in Randall's plaque formation. Mol Med. 2022;28(1):162.
28. Weigl M, Kocijan R, Ferguson J, et al. Longitudinal Changes of Circulating miRNAs During Bisphosphonate and Teriparatide Treatment in an Animal Model of Postmenopausal Osteoporosis. J Bone Miner Res. 2021;36(6):1131–44.
29. Gan L, Leng Y, Min J, et al. Kaempferol promotes the osteogenesis in rBMSCs via mediation of SOX2/miR-124-3p/PI3K/Akt/mTOR axis. Eur J Pharmacol. 2022;927:174954.
30. Gu N, Wang Y, Li L, et al. The mechanism of lncRNA MALAT1 targeting the miR-124-3p/IGF2BP1 axis to regulate osteogenic differentiation of periodontal ligament stem cells. Clin Oral Investig. 2024;28(4):219.
31. Li Z, Zhao H, Chu S, et al. miR-124-3p promotes BMSC osteogenesis via suppressing the GSK-3beta/beta-catenin signaling pathway in diabetic osteoporosis rats. In Vitro Cell Dev Biol Anim. 2020;56(9):723–34.